Chemical Engineering Journal 93 (2003) 135–142

Chemical Engineering Journal

www.elsevier.com/locate/cej

A model for pressure drop and liquid saturation in gas–liquid cocurrent upflow through packed beds

H. Sindhu, P.S.T. Sai*

Department of Chemical Engineering, Indian Institute of Technology, Chennai 600036, India

Accepted 26 August 2002

Abstract

A macroscopic model for pressure drop and liquid saturation in cocurrent gas–liquid upflow through packed beds was proposed. The three model parameters: two accounting for the effect of reduction in cross sectional area available for each phase due to the presence of the other, the third accounting for the effect of bubble formation were evaluated from the experimental data of the earlier investigation. The validity of the model for predicting the pressure drop was tested with an independent data reported in literature.

Keywords: Gas–liquid cocurrent; Countercurrent; Two-phase flow; Pressure drop; Liquid saturation

1. Introduction

Simultaneous gas and liquid flow through packed beds is commonly encountered in chemical processes for the transfer of energy or mass with or without chemical reaction between the phases. The flow of the phases can be countercurrent or cocurrent downwards or cocurrent upwards. While countercurrent is a mode of choice for mass transfer between the phases, cocurrent is for systems with chemical reactions. Cocurrent upflow provides high interfacial area and radial mixing of the phases, improved gas–liquid mass transfer coefficients and higher liquid saturation as compared to cocurrent downflow of the phases.

Several flow patterns appear in cocurrent gas–liquid upflow through packed beds depending upon the characteristics of the packing as well as the physical properties and flow rates of the two phases. The flow patterns for Newtonian non-foaming liquids are classified as: (i) bubble flow (BF) corresponding to low gas rates, characterized by continuous liquid flow and dispersed bubble flow; (ii) pulse flow (PF) corresponding to high gas rates and moderate liquid rates, characterized by liquid-rich and gas-rich portions passing through the column alternatively; and (iii) spray flow (SF) corresponding to high gas and low liquid rates wherein gas flowing continuously with liquid as film over the particles and partly as droplets in the gas phase.

Pressure drop and liquid saturation are two important design parameters in packed beds. Khan et al. [1,2] summarized the correlations proposed by earlier authors for pressure drop and liquid saturation in gas–liquid upflow through packed beds. These correlations are reported either in terms of Lockhart–Martinelli parameter or relating them to the bed characteristics and the Reynolds number defined separately for gas and liquid phases. Bensetiti et al. [3] proposed a state-of-the art correlation for the prediction of external liquid saturation on the basis of a large data bank consisting of more than 2600 experimental results published in the literature. Larachi et al. [4] derived a state-of-the art correlation for the prediction of frictional gas–liquid pressure drop in cocurrent upflow fixed bed reactors based on a wide hydrodynamic data bank of flooded packed bed reactors.

An analysis of the literature indicates that reliable correlations based on experiments exist for predicting the pressure drop and liquid saturation, but information on the modeling of the system is scarce. The complicated geometry and the fundamental difficulties in the theoretical description of fluid flow have made rigorous treatment difficult. The general approach has been semi-empirical through mathematical models based on analogy with simple systems.

Rao et al. [5] proposed a dynamic interaction model for pressure drop and liquid saturation in cocurrent downflow through packed beds within the framework of the momentum balance using the experimentally observed condition of no radial pressure gradients. The model includes the effect

Abbreviations: BF, bubble flow; PF, pulse flow; SF, spray flow

* Present address: School of Chemical Engineering, Engineering Campus, Universiti Sains Malaysia, 14300 Nibong Tebal, Seberang Perai Selatan, Pulau Pinang, Malaysia.
E-mail address: pstsmy@yahoo.com (P.S.T. Sai).

1385-8947/02/$ – see front matter
PII: S1385-8947(02)00226-7

Nomenclature

A	interfacial area (m^2)
d_0	orifice diameter (m)
d_p	effective particle diameter (m)
g	acceleration due to gravity ($m\,s^{-2}$)
G	gas superficial mass velocity ($kg\,m^{-2}\,s^{-1}$)
h	height of the packing (m)
L	liquid superficial mass velocity ($kg\,m^{-2}\,s^{-1}$)
ΔP	pressure drop ($N\,m^{-2}$)
ΔP^0	pressure drop for single phase ($N\,m^{-2}$)
S	free cross sectional area ($=(\pi D^2/4)\,\varepsilon$) ($m^2$)
V	superficial velocity of the phase ($m\,s^{-1}$)
V'	actual velocity of the phase ($m\,s^{-1}$)

Greek letters

α_B	non-ideality factor
α_G	Area of contact between gas and packing in two-phase flow to that in single-phase flow
α_L	area of contact between liquid and packing in two-phase to that in single-phase flow
β	total liquid holdup based on void volume
γ_G	dimensionless factor $(1-\gamma_L)$
γ_L	dimensionless factor $[=(L/\rho_L)/(L/\rho_L + G/\rho_G)]$
δ_{LG}	dimensionless frictional pressure drop $(=\Delta P_{FLG}/\rho_L gh)$
δ^0	dimensionless frictional pressure drop for single phase $(=\Delta P^0/\rho_L gh)$
ε	bed porosity
μ	viscosity ($kg\,m^{-1}\,s^{-1}$)
ρ	density ($kg\,m^{-3}$)
σ	surface tension ($N\,m^{-1}$)
τ	shear force
φ	energy dissipation ($N\,m\,s^{-1}$)
X	dimensionless factor $(=\sigma/\rho_L g d_0^2)$

Subscripts

F	frictional
G	gas phase
GW	gas packing
L	liquid phase
LG	liquid–gas
W	packing

of bubble formation on the pressure drop and liquid saturation and provides a functional form for correlating pressure drop and liquid saturation but some parameters have to be determined by fitting experimental data. They obtained the model parameters for air–water system. Sai and Varma [6] obtained these parameters for Newtonian non-foaming, Newtonian foaming and non-Newtonian systems in cocurrent gas–liquid downflow through packed beds.

In the present study, the above model is modified for conditions of upflow and the model parameters are obtained using the data reported in literature [7]. The pressure drop computed using these model parameters is compared with data reported by earlier investigators [8,9].

2. The model

A unified treatment based on the mechanical energy balance is presented using an internal flow model, based on analogy with flow through pipes, to describe the fluid dynamic aspects of cocurrent gas–liquid upflow through packed beds. The basic assumption in this treatment is that mass, momentum and energy balances apply in each phase. A simplified schematic diagram of the system is shown in Fig. 1.

Assuming isothermality, the integral momentum balance for the gas phase is as follows: [upward pressure force] − [downward pressure force] + [downward gravity force] = [total shear force between gas and liquid] + [total shear force between gas and packing]

$$\int_{\text{at } Z=0} (1-\beta)P\,\mathrm{d}S - \int_{Z=h} (1-\beta)P\,\mathrm{d}S + ghS(1-\beta)\rho_G = \int \tau_{LG}\,\mathrm{d}A_{LG} + \int \tau_{GW}\,\mathrm{d}A_{GW} \quad (1)$$

Similarly, for the liquid

$$\int_{\text{at } Z=0} \beta P\,\mathrm{d}S - \int_{Z=h} \beta P\,\mathrm{d}S + ghS\beta\rho_L = \int_{\text{at } Z=0} \tau_{LG}\,\mathrm{d}A_{LG} \int \tau_{GW}\,\mathrm{d}A_{LW} \quad (2)$$

Adding the two equations and writing ΔP for pressure difference between inlet and outlet gives the following equation for two-phase flow:

$$\Delta P_{LG} + [\beta\rho_L + (1-\beta)\rho_G]gh = \tau_{GW}\frac{A_{GW}}{S} + \tau_{LW}\frac{A_{LW}}{S} \quad (3)$$

It is assumed that ΔP is constant over the cross section and the shear stresses are constant over the entire area of contact for performing the integrations.

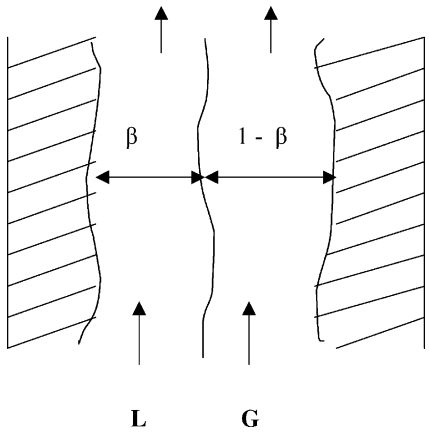

Fig. 1. Formulation of the flow of the phases.

The mechanical energy balance equation for the gas is given by

$$\Delta P_{LG}(1-\beta)SV'_G - ghS(1-\beta)\rho_G V'_G = \tau_{LG}A_{LG}V'_{iG} - \phi_G \quad (4)$$

Similarly, for the liquid

$$\Delta P_{LG}\beta SV'_L - ghS\beta\rho_L V'_L = -\tau_{LG}A_{LG}V'_{iL} - \phi_L \quad (5)$$

The rate of energy dissipation, ϕ, is related to τ_W in single phase as

$$\tau_W A_W = -\frac{\phi}{V'} \quad (6)$$

Assuming that there is no slip at the interface, Eqs. (4) and (5) can be added to give

$$\Delta P_{LG}[\beta V'_L + (1-\beta)V'_G] - [\beta\rho_L V'_L + (1-\beta)\rho_G V'_G]gh = -\frac{1}{S}(\phi_L + \phi_G) \quad (7)$$

Since the pressure drop for two-phase flow equals the pressure drop in each of the two phases, this equality for upward flow may be expressed as follows:

$$\Delta P_{LG} = \Delta P_L = \Delta P_G = \Delta P_{FL} + \rho_L gh = \Delta P_{FG} + \rho_G gh \quad (8)$$

Using this equation with along with equation Eq. (7) an expression for $(\phi_L + \phi_G)$ is

$$\Delta P_{FL}\beta V'_L + \Delta P_{FG}(1-\beta)V'_G = -\frac{1}{S}(\phi_L + \phi_G) \quad (9)$$

Expressing the frictional dissipation per unit area in terms of superficial mass velocities of gas and liquid and the frictional pressure losses of the individual phases

$$\Delta P_{FL}\frac{L}{\rho_L} + \Delta P_{FG}\frac{G}{\rho_G} = -\frac{1}{S}(\phi_L + \phi_G) \quad (10)$$

Substituting Eq. (10) in Eq. (7)

$$\Delta P_{LG}\left[\frac{L}{\rho_L} + \frac{G}{\rho_G}\right] - [L+G]gh = \Delta P_{FG}\frac{G}{\rho_G} + \Delta P_{FL}\frac{L}{\rho_L} \quad (11)$$

As per the geometric interaction model [5], the frictional pressure drop ΔP_{FG} for flow of gas due to the presence of liquid and bubble formation can be written as

$$\Delta P_{FG} = \frac{\Delta P^0_{FG}\alpha_G}{(1-\beta)^3} + 6\alpha_B\frac{\sigma}{d_0}\left[\frac{1.5\delta_{LG}^{-1}}{6\chi}\right]^{1/3}\frac{h}{d_p} \quad (12)$$

$$\frac{\Delta P_{FL}}{\Delta P^0_{FL}} = \frac{\alpha_L}{\beta^3} \quad (13)$$

$$\frac{\Delta P_{FG}}{\Delta P^0_{FG}} = \frac{\alpha_G}{(1-\beta)^3} \quad (14)$$

Two-phase pressure drop for upward flow is given by

$$\Delta P_{LG} = \Delta P_{FLG} + [\beta\rho_L + (1-\beta)\rho_G]gh \quad (15)$$

The terms of order ρ_G/ρ_L can be neglected in comparison with δ, the above equation reduces as follows:

$$\frac{\Delta P_{LG}}{\rho_L gh} = \delta_{LG} + \beta \quad (16)$$

where $\delta_{LG} = \Delta P_{FLG}/\rho_L gh$. Substituting for ΔP_{LG}, ΔP_{FG} and ΔP_{FL} of Eq. (11) from Eqs. (16), (12) and (13) respectively, the final equation obtained is as follows:

$$\delta_{LG} + \beta - \gamma_L - \gamma_G\frac{\rho_G}{\rho_L} - \gamma_G\left[\frac{\alpha_G\delta^0_G}{(1-\beta)^3} + \alpha_B(6\chi)^{2/3}(1.5\delta_{LG}^{-1})^{1/3}\frac{d_0}{d_p}\right] - \alpha_L\frac{\delta^0_L}{\beta^3}\gamma_L = 0 \quad (17)$$

where

$$\gamma_L = \frac{L/\rho_L}{(L/\rho_L) + (G/\rho_G)} \quad \text{and} \quad \gamma_G = 1 - \gamma_L$$

Substituting for ΔP_{LG} and ΔP_{FL} in Eq. (8), the final expression is as follows:

$$\delta_{LG} + \beta - \frac{\alpha_L\delta^0_L}{\beta^3} - 1 = 0 \quad (18)$$

Eqs. (17) and (18) are the final dimensionless expressions for pressure drop and liquid saturation.

The factor α_L and α_G are the ratios of the equivalent area of contact between the phases (liquid and gas, respectively) and packing in two-phase flow to that in a single-phase flow. The variable, α_B is a non-ideality factor accounting for the fact that in practice bubbles may not break or reform quite so often, and is expected to assume values between 0 and 1. At low liquid rates corresponding to spray flow, the liquid saturation is unaffected by the gas flow rate and thus $\alpha_L = 1$. This is true provided the gas flow rate is not too high to cause significant entrainment.

At intermediate and high liquid flow rates, the gas flow reduces the liquid saturation. At low gas flow rates corresponding to bubble flow, the formation and coalescence of bubbles result in filling up many of the voids, thus reduce the area of contact between liquid and packing when compared with single-phase flow. It is assumed that the reduction is equal to the liquid saturation itself, that is $\alpha_L = \beta$. The factor α_B should be maximum and lies between 0 and 1. The variables α_G and α_B are determined by fitting the experimental data with the model equations.

Alternate pulses of low density and high density characterize the pulse flow. The bubble formation in the high-density pulses reduces α_L, though the reduction is less than in bubble flow. The increased gas flow rate, however, causes spreading of the liquid film over a large area of packing. The effect of bubbles will be more significant in reducing α_L. By trial

and error, a value of 0.7 was assigned to give predictions with experiment. The values of α_G and α_B should be less than that for bubble flow, with the former being greater than 1. In summary, of the nine parameters, values are assigned a priori to three parameters as follows:

$\alpha_L = 1$ (spray flow);
$\alpha_L = 0.7$ (pulse flow);
$\alpha_L = \beta$ (bubble flow).

3. Results and discussion

The unknown parameters α_G and α_B for each of the identified flow regimes, i.e. spray flow, pulse flow and bubble flow are determined using the two-phase pressure drop data [7]. Using the experimental pressure drop, liquid saturation is calculated from Eq. (18). Then a linear least square analysis of Eq. (17) using experimental δ_{LG} and the calculated β gives the best values of constants α_G and α_B for each region. The values of α_G and α_B thus obtained are listed in Table 1 along with the values of α_L.

Once the parameters are estimated, δ_{LG} and β are calculated from input data on packing characteristics, fluid properties and flow rates of the two phases by solving Eqs. (17) and (18) using an iterative procedure. The details of this calculation as well as the method of parameter estimation are described in Appendix A.

The model is simulated for air–water and air–MEA systems in cocurrent upflow through a packed bed with different types of packing. The details of the experimental set-up are as stated by Khan [7]. The column and packing characteristics and physical properties used in the experiment are listed in Table 2.

Table 1
Model parameters obtained in the present study

Flow pattern	Model parameters		
	α_L	α_G	α_B
Spray flow	1.0	1.1961	0.0976
Pulse flow	0.70	1.2446	0.5757
Bubble flow	β	2.4534	0.8493

Table 3
Magnitude of different contributions to the total frictional pressure drop as predicted by the present model for typical mass flow rate of the phases, $d_p = 6.2$, $\varepsilon = 0.5$ and $D = 91.0$

L	G	Dimensionless pressure drop			Flow
		Geometric interaction		Contribution from bubble formation	
		Liquid phase	Gas phase		
43.564	0.841	0.3889	3.5404	1.5359	BF
41.727	0.841	0.3291	3.4553	1.5338	BF
39.122	0.577	0.3129	2.9401	0.9754	BF
34.851	0.521	0.2583	2.8522	0.9583	BF
24.430	0.124	0.1164	1.1360	0.8951	BF
17.596	1.029	0.0405	2.4966	0.7364	PF
17.596	0.239	0.0475	1.0216	0.2250	PF
8.542	0.577	0.0136	1.6677	0.5737	PF
26.138	1.029	0.1233	2.7276	0.8560	PF
39.122	0.978	0.3807	2.9977	0.8793	PF
8.542	0.773	0.0215	1.3499	0.1414	SF
8.542	0.611	0.0216	1.0122	0.1142	SF
10.677	0.611	0.0392	1.2095	0.1776	SF
6.406	0.521	0.0167	0.8419	0.0857	SF
10.677	0.577	0.0398	1.1179	0.1285	SF

The results of the simulation are presented in Table 3, and in Figs. 2 and 3. For the present study, the operating conditions as used by Rao et al. [5] for downflow are considered to make meaningful comparisons. Fig. 2 shows a plot of pressure drop versus gas flow rate for different liquid flow rates covering all regions of flow. Fig. 3 is similar plot for liquid saturation. In simulation the bed and column characteristics are $d_p = 6$ mm, $\varepsilon = 0.5$ and $D = 91$ mm. Each of these plots correspond to the whole range of operation of cocurrent upflow in terms of the variables liquid and gas flow rates. It is assumed in the theoretical development, that the region of operation is known a priori. The theoretical model for each region is then used to develop the curves shown in Figs. 2 and 3. Different lines, indicating the transition between regions, identify the flow regions.

Table 2
Input parameters to the model

Packing	Nominal size (mm)	Equivalent particle diameter (m)	Porosity
Packing characteristics			
Ceramic spheres	6.0	0.00620	0.39
Ceramic raschig rings	6.0	0.00600	0.48
Ceramic berl saddles	6.0	0.00857	0.62
Fluid	Density ($kg\,m^{-3}$)	Viscosity ($kg\,m^{-1}\,s^{-1}$)	Surface tension ($N\,m^{-1}$)
Physical properties of the fluids			
Water	1000	0.001	0.072
MEA	1020	0.015	0.049
Air	1.165	0.000018	–

Column characteristics: diameter (m), 9.1×10^{-2}; packing height (m), 1.0; liquid flow rate ($kg\,m^{-2}\,s^{-1}$), 1.067–46.00; gas flow rate ($kg\,m^{-2}\,s^{-1}$), 0.075–1.47.

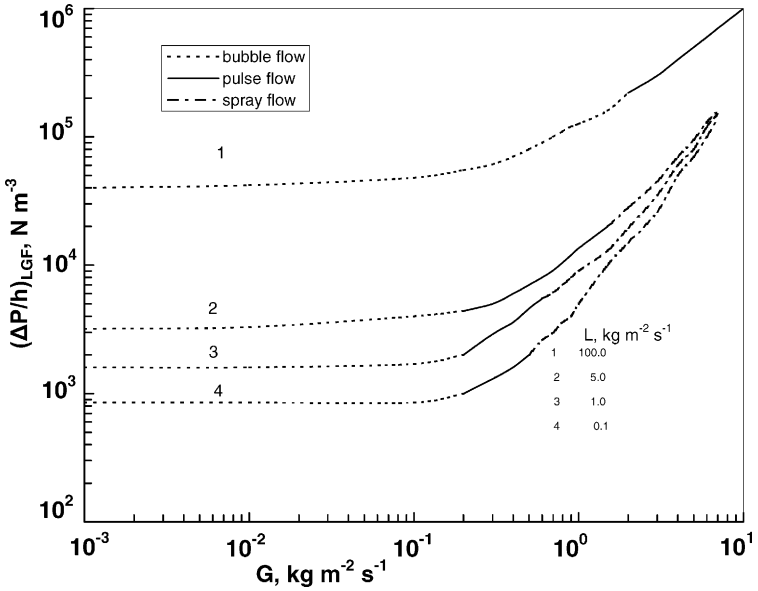

Fig. 2. Variation in pressure drop with mass flow rate of the phases as predicted by the present model.

At low liquid rates (e.g. $L = 0.1$), the flow pattern corresponds to bubble flow ($0 < G < 0.2$), pulse flow ($0.2 < G < 0.6$) and spray flow ($G > 0.6$). It is seen from the Fig. 2 that the calculated pressure drop is nearly independent of the gas flow rate for values $G < 0.2$. There is a step rise in pressure drop of the gas flow rate for values of $G > 0.2$. Fig. 3 shows the total liquid saturation at low liquid rates is similarly independent of the gas flow rate for $G < 0.5$. Thereafter, it decreases as gas flow rate increases.

At intermediate flow rates of the liquid ($L = 5$), the flow pattern corresponds to bubble flow ($0 < G < 0.2$), pulse flow ($0.2 < G < 1.5$) and spray flow ($G > 1.5$). In bubble flow region both the pressure drop and liquid holdup are nearly independent of the gas flow rate. In the pulse and spray flow regions, the pressure drop is increasing rapidly with an increase in gas flow rate while the liquid saturation decreases. The slope of the pressure drop curve is less in spray flow region indicating greater effect of the gas flow rate on the pressure drop on the latter region.

At high liquid rates ($L = 100$) flow pattern indicates the two major identified regions of flow, i.e. bubble flow ($0 < G < 1.6$) and pulse flow ($G > 1.6$). Figs. 2 and 3 show that in bubble flow region, both the pressure drop and liquid saturation are independent of gas flow rate for $G < 0.003$. Thereafter, as G is increased, the two phase pressure drop decrease at first slowly ($0.003 < G < 0.3$) and then rapidly ($G > 0.3$). For $G > 0.3$, the slope of the pressure drop curve is greater in pulse flow region

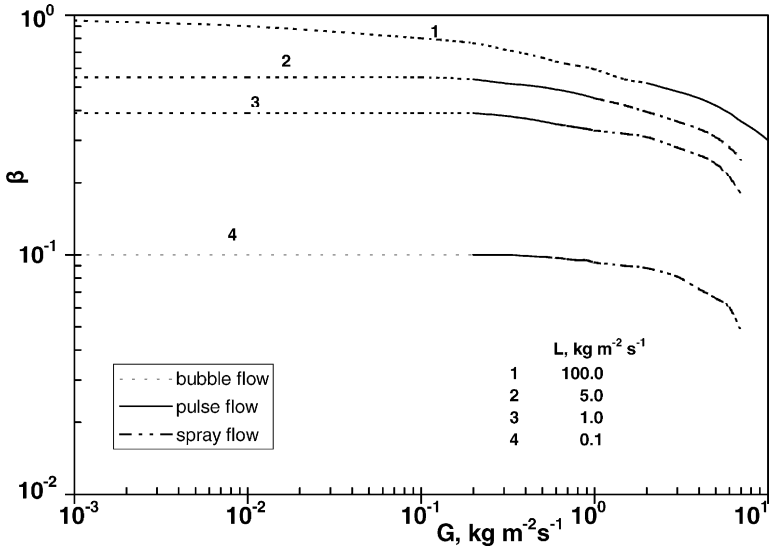

Fig. 3. Variation in liquid saturation with mass flow rate of the phases as predicted by the present model.

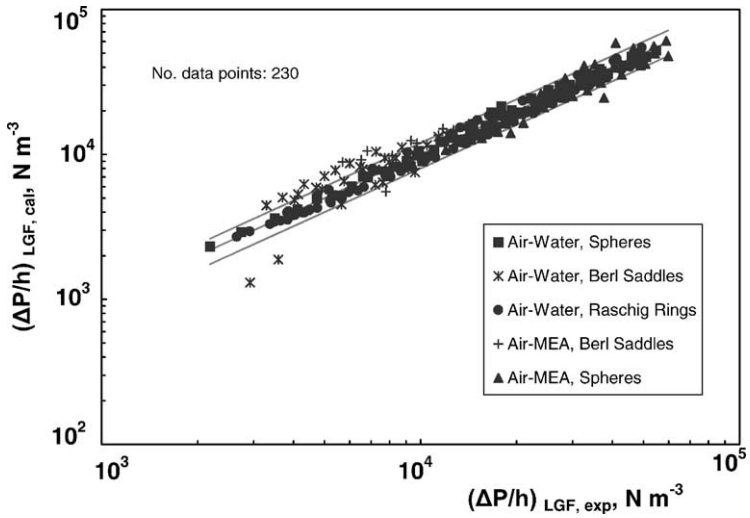

Fig. 4. Comparison of the two-phase experimental pressure drop data for bubble flow with data obtained using the present model.

than in bubble flow region indicating a greater effect of the two-phase pressure drop on the former region. These observations are, in general, same as that reported for downflow [5] excepting that the ranges are slightly different.

Figs. 4 and 5 compare the experimental two-phase pressure drop with the pressure drop predicted using the model for bubble flow and pulse flow respectively. The experimental liquid saturation is compared, typically for bubble flow, with that predicted using the model in Fig. 6.

Table 3 indicates the relative magnitude of different contributions to the total frictional pressure drop in two-phase flow for typical values of G and L in three different regions. It is clear that the contribution to the total pressure drop due to bubble formation may be small but significant in both bubble flow and pulse flow regions.

From the model it is predicted that the total pressure drop and liquid saturation are high for cocurrent upflow compared to cocurrent downflow. On comparison of α_B values for upflow with that of downflow, it is observed that the contribution towards total pressure drop due to bubble formation is more for upflow compared to that of downflow [5] indicating the reduction of the gas phase pressure drop due to geometric interaction. It is also observed that the contribution to the total pressure drop due to bubble formation is significant in both bubble flow and pulse flow regions and in spray flow region it is less compared to the other two regions. On the other hand, there is no significant variation in the values of α_L and α_G for upflow and downflow.

The validity of the present model is tested with experimental data obtained from two independent sources viz. Srinivas and Chhabra [8]and PERC [9]. While PERC [9] data covers low liquid rates and high gas rates thus yielding spray and pulse flows, the data due to Srinivas and Chhabra [8] cover high liquid rates and low gas rates yielding bubble and pulse flows. The experimental pressure drop data is

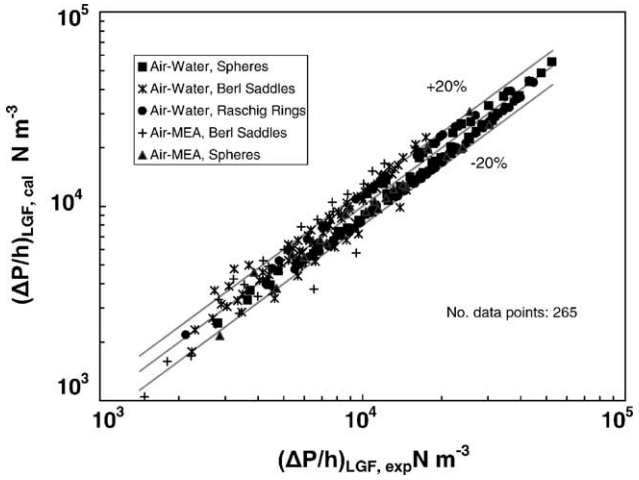

Fig. 5. Comparison of the two-phase experimental pressure drop data for pulse flow with data obtained using the present model.

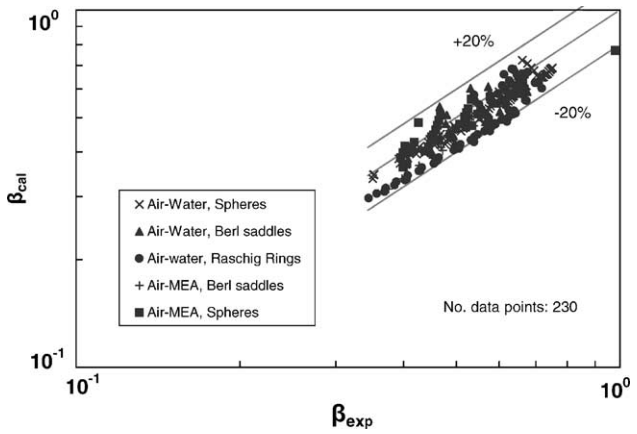

Fig. 6. Comparison of the two-phase experimental liquid saturation data for bubble flow with data obtained using the present model.

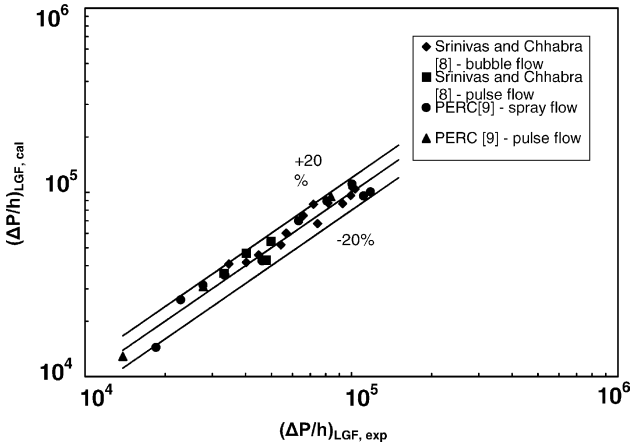

Fig. 7. Comparison of the literature two-phase experimental pressure drop data with data obtained using the present model.

compared with that predicted using the present model satisfactorily in Fig. 7.

4. Conclusions

The model, which was developed for cocurrent downflow, was modified to cocurrent upflow and satisfactorily predicts the pressure drop and liquid saturation. However, the model requires the knowledge of single-phase pressure drops and these are obtained using Ergun's equation [10]. The use of this expression alters the model parameters very lightly, but does not alter the overall agreement between the experiment and the model. This stresses the validity and merits of the present model.

Appendix A

The algorithm for the parameter estimation in the model is as follows.

1. Input the physical properties of gas and liquid (viscosity, density and surface tension).
2. Input the packing characteristics (porosity and effective particle diameter).
3. Read the experimental frictional pressure drop data with mass flow rate of the two phases.
4. Calculate single-phase pressure drop of the phases by using Ergun's equation.
5. Calculate the equivalent orifice diameter using the following equation:

$$d_0 = \frac{d_t - N d_p}{N} \tag{A.1}$$

where D is the column diameter and N an integer calculated as the integral part of (D/d_p) minus one;

6. Calculate the liquid saturation from Eq. (18) using MATLAB fsolve function. For finding initial guess to give input to the fsolve function, two values of β are guessed between 0 and 1 such that the function values of equation is in opposite sign, corresponding to these values. By linear interpolation between these values an approximate value of β is obtained. This β value can be used as an initial guess.
7. Since δ_{LG} and β are known, Eq. (17) is in the form $Y = \alpha_G X_1 + \alpha_B X_2$ where Y, X_1 and X_2 are known quantities. The present scheme for determining α_G and α_B assumes that α_L is known. This is necessary for using simple linear least square technique to determine α_G and α_B. However, α_L has been varied by assigning different values to it. The values of 1 and 0.7 for spray and pulse flow regions were arrived by selecting the best values of α_L. For bubble flow, α_L is assumed to be equal to the liquid saturation. Now, α_L is specified for all regions, α_G and α_B are to be determined for these regions. Y, X_1 and X_2 are calculated for all experimental data. The α_G and α_B are obtained by minimizing the sum of the squared deviations between the left and right-hand sides of the above equation.

The procedure for the direct calculation of δ_{LG} and β is as follows: once the parameters have been estimated, Eqs. (17) and (18) can be solved simultaneously for δ_{LG} and β, given the flow rates of the phases, the packing characteristics and the physical properties of the fluids.

1. Calculate the single-phase pressure drop of liquid (δ_L^0) and gas (δ_G^0) from Ergun's equation.
2. Calculate the orifice diameter using Eq. (A.1).
3. Identify the flow regime by following the equations proposed by Khan [7].

Transition from bubble flow to pulse flow

$$G^* = 0.19 + \frac{1.4 e^{0.15 L^*}}{500 + e^{0.15 L^*}}$$

where

$$G^* = G\left(\frac{1-\varepsilon}{\varepsilon}\right) \quad \text{and} \quad L^* = L\left(\frac{1-\varepsilon}{\varepsilon}\right)\left(\frac{\mu_L}{\mu_W}\right)^{0.33} \tag{A.2}$$

Transition from pulse flow to spray flow

$$G^* = 0.6 + 0.083 L \left(\frac{\mu_L}{\mu_W}\right)^{0.33} \tag{A.3}$$

4. Eq. (18) can be solved directly to give β as a function of δ_{LG} using the model for α_L

$$\begin{aligned} \text{bubble flow}: \beta &= \left[\frac{\delta_L^0}{\delta_{LG} + (\beta - 1)}\right]^{1/2} \\ \text{pulse flow}: \beta &= \left[\frac{0.7\delta_L^0}{\delta_{LG} + (\beta - 1)}\right]^{1/3} \\ \text{spray flow}: \beta &= \left[\frac{\delta_L^0}{\delta_{LG} + (\beta - 1)}\right]^{1/3} \end{aligned} \tag{A.4}$$

5. Eq. (17) can be written as an equation containing only δ'_{LG} as an unknown quantity by substituting the above result for β and using $(\delta'_{LG}\delta_{LG}+\beta)$ for δ_{LG}. The resulting equation is solved by fsolve function in MATLAB.

For finding initial guess, two values of δ'_{LG} are guessed such that the function values of the equation are in opposite sign corresponding to these values. A linear interpolation for $f = 0$ between these two values is used as initial guess input to fsolve function. From the calculated value of δ'_{LG} using Eq. (A.4), β value is calculated. Thus, δ_{LG} and β are estimated simultaneously.

References

[1] A. Khan, A.A. Khan, Y.B.G. Varma, Flow regime identification and pressure drop in cocurrent gas–liquid upflow through packed beds, Bioprocess Eng. 16 (1997) 355.
[2] A. Khan, A.A. Khan, Y.B.G. Varma, An analysis of the phase holdup in concurrent gas liquid upflow through packed beds using (I) drift-flux model, and (II) slip ratio, Bioprocess Eng. 22 (2000) 165.
[3] Z. Bensetiti, F. Larachi, B.P.A. Grandjean, G. Wild, Liquid saturation in cocurrent upflow fixed-bed reactors: a state-of-the-art correlation, Chem. Eng. Sci. 52 (1997) 4239.
[4] F. Larachi, A. Laurent, G. Wild, N. Midoux, Some experimental liquid saturation results in fixed bed reactors operated under elevated pressure in cocurrent upflow and downflow of the gas and the liquid, Ind. Eng. Chem. Res. 30 (1991) 2404.
[5] V.G. Rao, M.S. Ananth, Y.B.G. Varma, Hydrodynamics of two-phase concurrent downflow through packed beds, AIChE J. 29 (1983) 467.
[6] P.S.T. Sai, Y.B.G. Varma, Pressure drop in gas–liquid downflow through packed beds, AIChE J. 33 (1987) 2027.
[7] A. Khan, Flow pattern of the phases, phase holdup and pressure drop in concurrent gas–liquid upflow through packed beds, Ph.D Thesis, Indian Institute of Technology Madras, India, 1998.
[8] K.V. Srinivas, R.P. Chhabra, Pressure drop in two-phase cocurrent upward flow in packed beds, Can. J. Chem. Eng. 72 (1994) 1085.
[9] Pittsburgh Energy Research Centre (PERC) quarterly report 1975–1976 (as cited in Y.T. Shah, Dynamics of the cocurrent upflow fixed-bed column, in: Gas–Liquid–Solid Reactor Design, McGraw-Hill, New York, USA, 1979, p. 230.)
[10] Ergun, Fluid Flow Through Packed Columns, Chem. Eng., Prog. 48 (1952) 89.